Plant Growth Regulation (2025) 105:1105–1123
https://doi.org/10.1007/s10725-025-01322-6

ORIGINAL PAPER

Physio-biochemical and dynamic transcriptome comparison of heat tolerance in wild and cultivated tomato accessions

Chunmei Shi[1] · Bo Liu[1] · Lei Song[1] · Yunfei Tang[1] · Jiawei Chen[1] · Xinyan Shen[1] · Yuxin Peng[1] · Can Yang[1] · Guangyu Lu[1] · Xuan Deng[1] · Yongen Lu[1] · Michal Lieberman-Lazarovich[2] · Bo Ouyang[1]

Received: 11 September 2024 / Accepted: 16 March 2025 / Published online: 23 April 2025
© The Author(s) 2025

Abstract

Tomato, one of the most important vegetable crops around the world, is sensitive to heat stress. Identifying heat-tolerant genes and breeding resilient varieties are vital for addressing the challenges of global warming and ensuring food security. In this study, we compared seedlings of a cultivated tomato accession (*Solanum lycopersicum*, M82) with those of a wild accession (*S. pimpinellifolium*, LA1589) at both physio-biochemical and transcriptomic levels under a 42℃ heat treatment. Various physio-biochemical indicators demonstrated that LA1589 exhibited superior heat tolerance compared to M82 at the seedling stage. We conducted dynamic transcriptome analyses of these two genotypes under heat treatment, identifying 10,681 differentially expressed genes (DEGs) in LA1589 and 10,462 DEGs in M82. Among these, 1,857 genes were specifically up-regulated and 1,228 genes were specifically down-regulated in LA1589, while 1,916 genes were specifically up-regulated and 1,021 genes were specifically down-regulated in M82. The enrichment analyses indicated that DEGs were significantly clustered in biological processes and pathways associated with heat resistance. Notably, the specifically down-regulated genes in LA1589 were significantly enriched only in the plasma membrane pathway, whereas in M82, these genes were enriched in chloroplast-associated processes and other pathways. Weighted gene co-expression network analysis identified heat-response modules, including TM11, PM3 and PM23. Further analysis revealed the involvement of *SlHsfA7*, heat shock proteins and chloroplast-related genes in the center of the heat-responsive regulatory network in tomato. Our findings provide a solid foundation for further functional elucidation of candidate heat-tolerant genes and their underlying molecular mechanisms in tomato.

Keywords Tomato · Heat stress · Dynamic transcriptome · Hub gene

Abbreviations

HS	Heat stress
REC	Relative electrical conductivity
CC	Chlorophyll content
MDA	Malondialdehyde
SOD	Superoxide dismutase
POD	Peroxidase
CAT	Catalase
F_v/F_m	Maximum quantum yield
PBS	Phosphate buffered saline
DEG	Differentially expressed gene
FPKM	Fragments Per Kilobase of transcript per Million mapped reads
PCC	Pearson correlation coefficient
PCA	Principal component analysis
PCG	Protein coding gene
WGCNA	Weighted gene co-expression network analysis
TF	Transcription factor
GO	Gene Ontology
KEGG	Kyoto Encyclopedia of Genes and Genomes
BP	Biological process
H_2O_2	Hydrogen peroxide
PSII	Photosystem II
HSF	Heat shock factor
HSP	Heat shock protein

Chunmei Shi and Bo Liu have contributed equally to this work.

✉ Bo Ouyang
bouy@mail.hzau.edu.cn

[1] National Key Laboratory for Germplasm Innovation and Utilization of Horticultural Crops, College of Horticulture and Forestry Sciences, Huazhong Agricultural University, Wuhan 430070, China

[2] Plant Sciences Institute, Agricultural Research Organization Volcani Center, 7505101 Rishon LeZion, Israel

Introduction

With the increasing global temperatures and the prevalence of heat waves, heat stress (HS) has become a major constraint on crop production. Global temperatures are predicted to rise by 1.5–2°C by 2040 (IPCC, 2023). It has been observed that for every 1°C increase in the global average temperature, crop yields for major crops decrease by an average of 3.1%–7.4% (Zhao et al. 2017).

Heat stress can cause significant damage to plants, during both the vegetative and reproductive growth stages. During the vegetative growth stage, HS can lead to delayed plant development, leaf shedding, inhibited shoot and root growth, and reduced productivity (Bita and Gerats 2013). In the reproductive stage, HS can alter the morphology of plant anthers, reduce pollen quantity and viability, decrease fruit set rate, and result in yield losses (Kumar et al. 2017; Bheemanahalli et al. 2019; Liu et al. 2019). Numerous studies have demonstrated that HS during the reproductive stage is more severe when compared to the vegetative stage. In particular, during the flowering stage, minor temperature fluctuations may not significantly impact vegetative growth and photosynthesis activities, but can substantially affect flower development and reduce the fruit set rate (Hedhly 2011; Lohani et al. 2020).

Tomato is one of the most important vegetables in the world, but it is highly sensitive to HS. Tomato fruits are rich in essential nutrients and antioxidants, such as vitamins A and B, flavonoids, lycopene, and ascorbic acid (Choudhary et al. 2013). The optimal temperature range for tomato growth is 13°C–30°C. When the daytime temperature exceeds 32°C, tomato plants experience HS, and beyond 35°C, their growth and development are severely compromised, leading to leaf wilting, pollen sterility, reduced seed production, and decreased fruit set rate (Pham et al. 2020; Rahmat et al. 2023; Mubarok et al. 2019). With the rise in global temperatures, instances of tomato yield reduction due to extreme high temperatures are increasing. Therefore, breeding heat-tolerant tomato varieties has become an inevitable strategy to ensure the stability of the tomato industry (Mubarok et al. 2019; Aldubai et al. 2022).

To develop heat-tolerant tomato varieties, it is crucial to identify heat-tolerant germplasm and genes. Heat tolerance, being a quantitative trait, requires the consideration of multiple factors in its assessment (Wen et al. 2019). Various indicators have been used to identify heat-tolerant materials, such as relative electrical conductivity (REC), proline, and chlorophyll content (CC) (Rajametov et al. 2021; Zhou et al. 2015). Bhattarai et al. (2021) utilized chlorophyll fluorescence, CC, plant height, stem diameter, leaf temperature, and electrolyte leakage to screen several heat-tolerant lines, including Heat Master, New Girl, and HM-1823. Similarly, LA1500 and LA2093 were selected based on photosynthetic parameters, pollen viability, and CC. Driedonks et al. (2018) identified Nagcarlang, Hotset, and Saladette as heat-tolerant materials by examining reproductive-stage traits, such as pollen vigor and quantity. However, due to the lack of consistency in the indicators used by different studies, there may be a lack of robust indicators to reliably confirm the heat resistance of identified materials. As a result, further verification is often necessary for materials identified as heat-resistant. In our comprehensive review of previous research, we have justified several key indicators for evaluating tomato heat tolerance, including malondialdehyde (MDA), REC, various antioxidant enzymes, CC, and maximum quantum yield (F_v/F_m) (Liu et al. 2023).

RNA-seq technology has proven to be a valuable tool for identifying stress-resistant genes. In the context of heat tolerance, researchers have utilized RNA-seq to study gene expression and response networks in wheat under HS, providing insights into the physiological and molecular regulatory mechanisms of thermotolerance (Azameti et al. 2022). Similarly, this technology has been employed to investigate the dynamic transcriptional changes in maize leaves, pollen, and embryos under HS, leading to the identification of potential candidate genes for heat-tolerant maize breeding (Jagtap et al. 2023). Transcriptome analysis of heat-tolerant and heat-sensitive genotypes of cabbage under HS has revealed potential heat-tolerant genes and shed light on response mechanisms to HS (Ikram et al. 2022). In addition, RNA-seq data have demonstrated that *HsfA1a* enhances heat tolerance and cellular homeostasis in Arabidopsis pollen under HS by boosting antioxidant capacity, protein repair, and degradation (Xie et al. 2022). In tomato, transcriptome analysis of plants subjected to HS and nitrogen fertilizer treatments has indicated that nitrogen fertilization improves the heat tolerance of young tomato fruits through enhanced sugar metabolism under HS (Zheng et al. 2023). Mizoi et al. (2023) identified variations in gene expression between heat-tolerant and heat-sensitive tomato cultivars through transcriptome analysis, and specific heat-responsive biomarker genes were selected as candidate markers to evaluate heat tolerance in different tomato cultivars. Overall, RNA-seq technology plays a crucial role in plant heat-tolerance research, enabling the identification of candidate genes and the elucidation of adaptive mechanisms under HS. However, there is currently a lack of reports on dynamic transcriptome studies of heat-tolerant and heat-sensitive genotypes in tomato.

The aim of this study was to compare the differences in heat tolerance at the seedling stage between two tomato genotypes, LA1589 and M82. First, we assessed important physiological and biochemical indicators associated with

heat tolerance. Then, based on these findings, we employed RNA-seq technology to generate dynamic transcriptomic data for both genotypes, identifying differentially expressed genes (DEGs) under HS and comparing the differences in regulatory pathways between them. Furthermore, by utilizing weighted gene co-expression network analysis (WGCNA), we obtained heat response modules and constructed corresponding co-expression networks of hub genes, thereby examining the similarities and differences in the heat response mechanisms of LA1589 and M82. Our study has identified numerous critical heat-tolerant candidate genes for tomato, and offers insights into the molecular mechanisms underlying tomato heat tolerance.

Materials and methods

Plant growth conditions and treatment

Tomato seedlings of M82 (*Solanum lycopersicum*) and LA1589 (*S. pimpinellifolium*) were cultivated in a growth chamber at 25°C, with a relative humidity of 60–65%, and a photoperiod of 16 h light/8 h darkness. When the seedlings reached 28 days old, they were exposed to HS treatment at 42°C. The third leaf, which possesses a high photosynthetic capability, was harvested at 0, 3, 6, 12 and 24 h during heat treatment for the measurement of stress-related parameters. Similarly, the same positional leaves were collected at 0, 0.5, 1.5, 3, 6, 12, 24 h during exposure to 42°C, and at 24 h after recovery at 25°C for transcriptome analysis. Fresh samples were immediately cut and used for the determination of REC and F_v/F_m. All other samples were promptly frozen in liquid nitrogen after collection and stored at − 80°C for RNA extraction.

Measurement of REC

The REC value of tomato leaves was determined according to a published method (Cao et al. 2007). The leaves were washed three times with deionized water and sliced. Approximately 0.05 g of leaf samples were weighed before being immediately transferred to a centrifuge tube containing 10 ml of deionized water. The leaf sample was then vacuumed and permeated for 15 min, followed by an incubation of 2 h at room temperature. Subsequently, the electrical conductivity (EC1) was measured using a DDB-303 portable conductivity meter (Leici Instrument Co. Ltd., Shanghai, China). The leaves were then boiled for 30 min, allowed to cool to room temperature, and the electrical conductivity value (EC2) for the solution was measured. REC was calculated as follows: REC (%) = EC1/EC2 × 100%.

Determination of antioxidant enzyme activity and MDA content

The crude enzyme solution for measuring antioxidant enzyme activity was extracted following published protocols (Hu et al. 2019). Leaf samples were ground in liquid nitrogen, and 0.1 g of the sample was added to a 2 ml Eppendorf tube. Then, 2 ml of pre-cooled 50 mM phosphate-buffered saline (PBS) solution (pH 7.8) was added. After vortexing, the extracts were centrifuged at 12,000 rpm for 10 min at 4°C. The supernatant was used to determine the activity of superoxide dismutase (SOD), peroxidase (POD), and catalase (CAT).

SOD activity was measured using the nitrogen blue tetrazole (NBT) method (Beyer and Fridovich 1987). A mixture was prepared based on the number of samples tested. For each well of the microplate, 50 µL of crude enzyme extract and 200 µL of mixture were added, with a blank control set using an equal amount of 50 mM phosphate buffer (pH7.0). The microplate was placed in an incubator for 20 min. Subsequently, the absorbance at 560 nm was measured using a microplate reader (Infinite 200 Pro, Tecan, Mannedorf, Switzerland). The SOD activity was calculated using the formula: SOD (U/mg FW) = $[(A_{CK}-A_E) * V_T]/(A_{CK} * 0.5 * W * V_S)$.

POD activity was determined using the guaiacol oxidation method (Chakraborty et al. 2015). Similarly, 10 µL of crude enzyme extract and 100 µL of mixture buffer were added into each well. After an incubation for 1 min, the reaction was stopped by adding 50 µL of 1 mM H_2SO_4. The absorbance value at 470 nm was then measured. The POD activity was calculated using the formula: POD (U/(mg·min) FW) = $(A_E-A_{CK}) * V_T/(W * V_S * T)$. In the above formulas, V_T is the total volume of crude enzyme solution (mL); Vs is the amount of enzyme solution added (50 µL); W is the fresh weight of leaf sample (mg); A_{CK} is absorbance value of control; A_E is the absorbance value of sample; T is the time of reaction.

CAT activity and MDA content were measured using corresponding commercial kits (Jiancheng Bioengineering Institute, Nanjing, China).

Measurements of CC and chlorophyll fluorescence

CC was determined following the method of (Wang et al. 2016). Leaves were ground in liquid nitrogen, and 0.1 g of the sample powder was placed into a 2 mL Eppendorf tube. Then 2 mL of 95% ethanol was added, and the extraction process was carried out in darkness for 24 h until the sample powder turned white. Subsequently, the extracts were centrifuged at 3000 rpm for 5 min before measurement, with 95% ethanol used as a blank. The absorbance values of the chlorophyll extract at 646 nm and 663 nm were recorded

using the microplate reader. The chlorophyll contents were calculated as follows:

$$\text{Chl a(mg/L)} = 12.21A_{663} - 2.81A_{646}$$

$$\text{Chl b (mg/L)} = 20.13A_{646} - 5.03A_{663}$$

$$\text{Total chlorophyll(mg/L)} = \text{Chl a} + \text{Chl b}$$

Chlorophyll fluorescence imaging was performed using a Maxi-Imaging-PAM chlorophyll fluorescence analyzer (Walz, Effeltrich, Germany), and the F_v/F_m values were recorded for both tomato genotypes (Murchie and Lawson 2013).

RNA extraction

RNA was extracted using TRIzol reagent (Invitrogen, Carlsbad, CA, USA) following the product manual. Tissue was ground in liquid nitrogen, extracted with TRIzol, and then centrifuged. The resulting supernatant was transferred to a new tube and purified with chloroform. Isopropyl alcohol was added to precipitate the RNA sample. After centrifugation, the RNA pellet was washed with ethanol, dried, and finally dissolved in DEPC-treated water.

Transcriptome analysis

A total of 48 leaf samples were collected from eight time points of LA1589 and M82, namely L1-L8 and M1-M8 (with three biological replicates), and sent to Novogene Co., Ltd. (Beijing, China) for library construction. Transcriptome sequencing was then performed on Illumina's HiSeq4000 platform (San Diego, CA, USA) using the PE150 sequencing strategy. Raw reads were filtered using Fastp software (Chen et al. 2018), and the resulting clean reads were aligned to the tomato reference genome SL2.50 (http://solgenomics.net/) using Hisat2 software (Kim et al. 2019). All uniquely aligned reads were extracted and converted into compressed, sorted BAM files using SAMtools (Li et al. 2009). Gene quantification was performed using featureCounts (Liao et al. 2014) to obtain a gene expression quantification matrix (counts matrix). The FPKM (Fragments Per Kilobase of transcript per Million mapped reads) method was used in this study to estimate mRNA expression levels, aiming to eliminate differences in gene expression levels caused by gene length and sequencing depth. Genes with an average FPKM ≥ 1 in biological replicates were considered expressed. For quality control of the samples, the FPKM values of all genes were transformed to log2(FPKM + 1), and then Pearson correlation coefficients (PCCs) were calculated using the built-in function"cor"in R to assess the biological reproducibility among pairwise samples. A heatmap of the PCC was generated using the R package"corrplot". In addition, principal component analysis (PCA) was performed using the R package "prcomp" to cluster different samples. Hierarchical clustering of all genes based on log2(FPKM + 1) values was conducted using the R functions "dist" (method ="Euclidean") and"hclust"(method ="average").

Identification of differentially expressed genes (DEGs)

Differential gene expression analysis was performed based on the obtained counts matrix using DESeq2 (Wang et al. 2010). Genes with a |log2(Fold Change)| ≥ 1 and a false discovery rate (FDR) < 0.05 were considered DEGs (Love et al. 2014). These DEGs were classified into several groups based on their expression patterns, including specifically up-regulated/down-regulated (only at one time point), variably up-regulated/down-regulated (at 2–6 time points), commonly up-regulated/down-regulated (at all 7 time points), and complex patterns (genes that were up-regulated at one time point but down-regulated at another).

Weighted gene co-expression network analysis (WGCNA)

WGCNA was conducted using the corresponding R package (Langfelder and Horvath 2008). Genes with FPKM ≥ 5 in at least one sample and a high coefficient of variation (CV > 0.5) were included. The "pickSoftThreshold" function was utilized to choose the power value, and the network was constructed in a one-step manner using the "blockwiseModules" function. The built-in "TOMsimilarity"algorithm was employed to calculate the Topological Overlap Matrix (TOM), and hierarchical clustering was performed using the dynamicTreeCut package (v1.63–1) to divide genes into modules. PCA analysis was conducted on all genes within each module, and the first PCA value represented the Module Eigengene (ME), indicating the overall level of gene expression within the module. The Eigengene-based connectivity (KME) was calculated using the "signedKME" function to measure the correlation between genes and modules, with genes having KME ≥ 0.9 identified as hub genes in the network. The results of WGCNA were visualized using Cytoscape software (Doncheva et al. 2019).

Gene ontology (GO) and KEGG analysis

All the DEGs were mapped to the terms in the GO database (http://geneontology.org/) and the number of genes for each term was calculated. Hypergeometric testing with a filtering criterion of q-value < 0.05 was then applied to identify significantly enriched GO terms in the analyzed genes compared to the background of the entire genome. KOBAS3.0

was used for annotation and enrichment analysis of DEGs for the Kyoto Encyclopedia of Genes and Genomes (KEGG) pathways, with a p-value < 0.05 as the criterion (Bu et al. 2021).

Reverse transcription quantitative PCR (RT-qPCR)

To validate the reliability of the RNA-seq data, four genes, inculding *SlHSP20.1* (Solyc11g020040), *SlHSP70* (Solyc09g065660), *SlHSFA7* (Solyc02g083850), and *CPK28* (Solyc06g076540), from the common DEGs between the two genotypes, were selected for RT-qPCR validation. Primers were designed using Primer5 and the primer design tool on the NCBI website (https://www.ncbi.nlm.nih.gov/tools/primer-blast) (Supplemental Table S13). The cDNA was synthesized using HiScriptII 1st Strand cDNA Synthesis Kit with genomic DNA wiper (Vazyme, Nanjing, China) according to the supplier's instruction. The 10 µL qPCR reaction contains 5 µL of SYBR premix Ex Taq (TransGen Biotech Co., Ltd., Beijing, China), 4 µL of cDNA, and 0.5 µL each forward and reverse primer. The amplification was performed on QuantStudio 7 (Thermo Fisher Scientific). The qPCR program is set as follows: pre-denaturation at 95℃ for 1 min, followed by 40 cycles of 95℃ for 10 s, 55℃ for 15 s, and 72℃ for 20 s. For each sample, three biological replicates and three technical replicates were performed. The expression levels of the DEGs were calculated using the $2^{-\Delta\Delta Ct}$ method (Schmittgen and Livak 2008). Actin (Supplemental Table S13) was used as the reference gene (Liu et al. 2020a).

Results

Effects of heat stress on phenotype and antioxidant enzyme activity

To evaluate the thermotolerance of LA1589 and M82, four-week-old seedlings were exposed to a 42°C HS. After 24 h, M82 exhibited more pronounced wilting than LA1589. Following 24 h of recovery at 25°C, LA1589 largely recovered, while M82 still displayed symptoms of leaf wilting (Fig. 1A).

We measured the activity of several antioxidant enzymes and found that CAT activity in LA1589 was consistently higher than in M82, both before and after heat treatment, with activity levels 1.2 to 1.4 times higher than those in M82 (Fig. 1B). In addition, there was no significant difference in SOD activity between the two genotypes before heat treatment. Upon 6 h of HS, both genotypes showed a substantial decrease in SOD activity, but LA1589 maintained significantly higher SOD activity than M82, at 1.68 times the level observed in M82 (Fig. 1C). After 24 h of HS, SOD activity in LA1589 remained relatively high, 1.48 times higher than in M82. The POD activity of LA1589 under heat treatment was significantly higher than that of M82 only at 12 h of HS, while at other time points, it was only slightly higher than in M82 (Fig. 1D).

Changes in MDA content and REC in the two genotypes under heat stress

Under HS, toxic substances such as MDA and ROS are typically produced, leading to cell membrane damage and electrolyte leakage (Yu et al. 2019). Therefore, we analyzed the changes in MDA content and REC levels in LA1589 and M82 during HS. Initially, no significant differences in MDA content and REC were observed between the two tomato genotypes prior to heat treatment.

During the early stages of HS, both genotypes exhibited an increasing trend in REC. However, as the stress persisted, the REC in M82 first decreased and then increased, while it continued to decrease in LA1589. Following 24 h of HS, the REC in M82 increased by 85.77%, whereas in LA1589, it only showed a more modest increase (by 20.18%). At this time point, the REC in M82 was 1.61 times higher than in LA1589 (Fig. 1E).

While the MDA content of both genotypes continued to rise after HS, it increased by 23.46% in M82 after 6 h of HS, whereas it remained unchanged in LA1589. After 24 h of HS, the MDA content of LA1589 and M82 increased by 36.74% and 98.62%, respectively, however, the disparity between the two genotypes was found to be statistically insignificant (Fig. 1F).

Effects of heat stress on photosynthesis

We measured CC and F_v/F_m, which are two critical indicators of photosynthetic capacity. Before HS, there was no difference in CC between LA1589 and M82. After 6 h HS, CC increased by 28.14% in LA1589, whereas in M82, the increase was only 9.89%. Following 12 h HS, CC in LA1589 increased by 18.93%, while in M82, it returned to the pre-HS level (Fig. 1G). Chlorophyll fluorescence imaging showed that after 6 h of HS, chlorophyll fluorescence decreased in both genotypes, but the decrease was less pronounced in LA1589 than in M82. After 24 h of HS, F_v/F_m decreased by 5.5% and 7.3% in LA1589 and M82, respectively (Fig. S1).

Dynamic changes in transcriptome of LA1589 and M82 under HS

To investigate the heat response mechanism of tomato plants and identify heat-tolerant genes, we conducted transcriptome sequencing on the 48 leaf samples (with

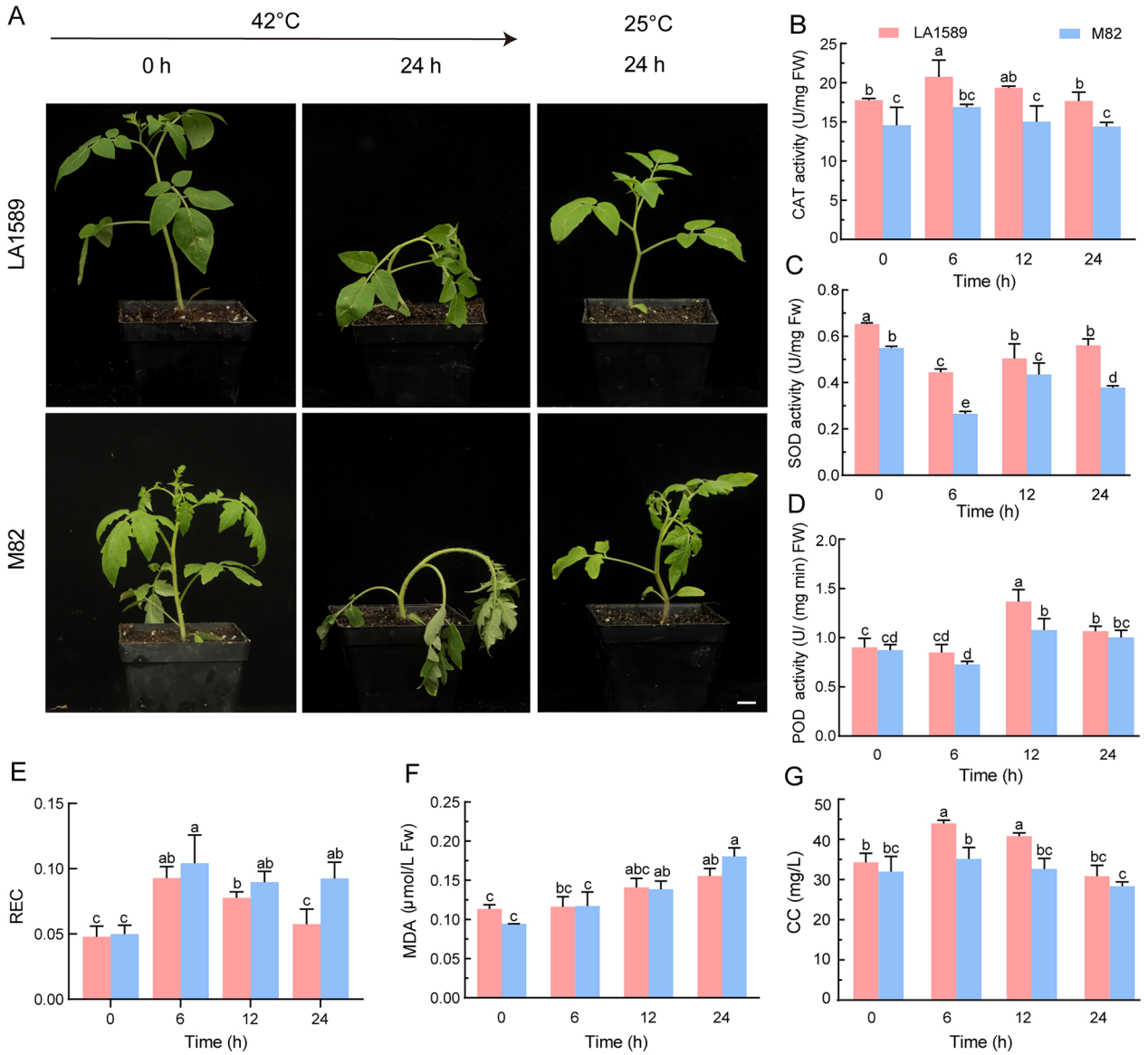


Fig. 1 Heat tolerance identification of LA1589 and M82. **A** Phenotype of four-week-old tomato plants under heat stress for 0 h, 24 h, and recovery at 25°C for 24 h. Scale bar = 1 cm. **B–G** Bar graphs of related physiological and biochemical indicators: Catalase (CAT) activity (**B**), Superoxide dismutase (SOD) activity (**C**), Peroxidase (POD) activity (**D**), Relative electrical conductivity (REC) (**E**), Malondialdehyde (MDA) content (**F**), Chlorophyll content (CC) (**G**). Data are presented as mean ± standard deviation of three biological replicates. Data were analyzed using one-way ANOVA followed by Duncan's multiple range test. Different letters indicate significantly different at $P < 0.05$

three biological replicates) from LA1589 and M82. These samples were collected at various time points (0, 0.5, 1.5, 3, 6, 12, 24 h) under 42°C HS, followed by a 24-h recovery period at 25°C. Each time point was labeled as L1-8 for LA1589 and M1-8 for M82 samples, respectively. We obtained raw reads ranging from 39.29 to 91.37 millions for each sample, and after filtering, the clean reads ranged from 39.12 to 90.95 millions. The average GC content was 45.48% (Table S1), confirming high-quality sequencing data, which is suitable for further analysis. After mapping clean reads to the tomato reference genome (SL2.50), the total alignment rate averaged 92.72%, with 90.72% unique alignment (Table S1). These results confirm the reliability of the sequencing data for subsequent analysis. Gene expression quantification was performed based on the alignment results, using normalized expression values (FPKM values) to represent gene expression levels. To ensure consistency of biological replicates, we removed outlier samples using Pearson correlation coefficient (PCC), principal component analysis (PCA),

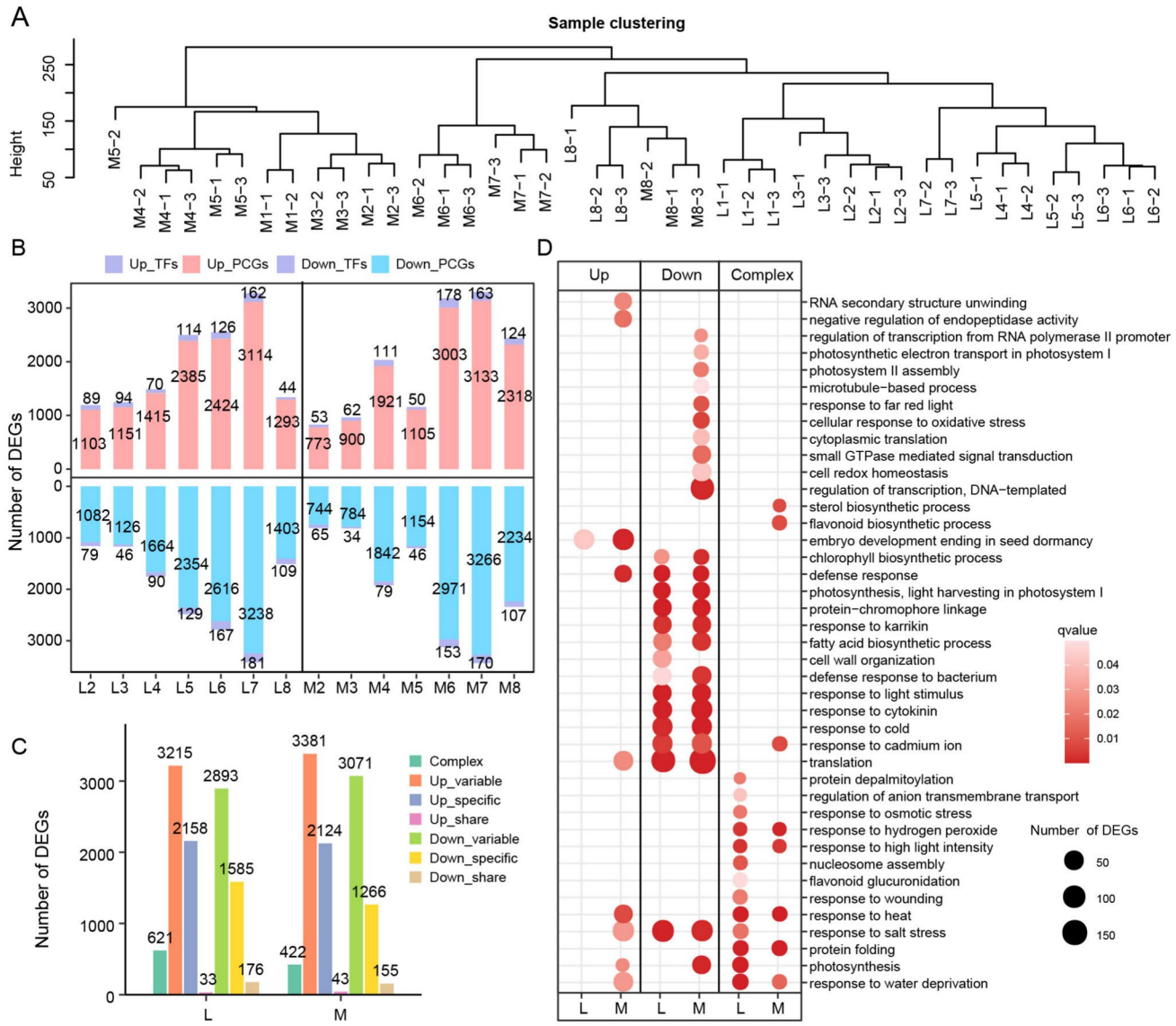


Fig. 2 Differentially expressed genes (DEGs) identified in LA1589 and M82 during heat stress and recovery. **A** Sample clustering based on log2-transformed (FPKM +1) values of all expressed genes."M" and "L" represent M82 and LA1589, respectively. The numbers before the "-" indicate time points at 0, 0.5, 1.5, 3, 6, 12, and 24 h of heat stress treatment at 42°C and 24 h of recovery at 25°C. The numbers following the "-" represent biological replicates. **B** Number of DEGs in LA1589 and M82 at each time point. Red, blue and purple indicate up-regulated protein-coding genes (PCGs), down-regulated PCGs, and transcription factors (TFs), respectively. **C** Number of categorized DEGs under different time points. Complex (genes were up-regulated at one time point but down-regulated at another). Specific DEGs (differentially expressed under one time point), variable DEGs (differentially expressed under two to six time points) and shared DEGs (differentially expressed under seven time points). **D** Representative gene ontology (GO) terms of DEGs in LA1589 and M82. The circle size indicates the number of DEGs associated with each GO term, with larger circles representing higher enrichment. The color intensity represents the q-value, with deeper red indicating more reliable significance of DEG enrichment in the pathway. All significantly enriched GO terms (q-value <0.05) in each time point are listed in Table S4. Up (genes were up-regulated at least at one time point), Down (genes were down-regulated at least at one time point), and Complex (genes were up-regulated at one time point but down-regulated at another)

and hierarchical clustering. This resulted in 43 samples remaining for further analysis (Fig. 2A, Fig. S2). PCC and PCA results showed good clustering of biological replicates, with the first and second principal components explaining 32.9% and 15.1% of the variation, respectively (Fig. S2B). The clustering analysis also revealed distinct groups for M82 and LA1589 samples (Fig. 2A). With reliable samples and data, we conducted transcriptome analysis to identify heat-responsive genes.

To investigate changes in gene expression levels over time, we identified DEGs in the heat-tolerant genotype LA1589 and the heat-sensitive genotype M82 (Table S3). By comparing each treatment with the control (0 h), we observed varying numbers of DEGs at different time points. Generally, the number of DEGs increased with prolonged HS, except for the M5 time point in M82. The number of DEGs significantly decreased after recovery at normal temperature (Fig. 2B, Fig. S3). At each time point, a certain number of transcription factors (TFs) were up-regulated or down-regulated (Fig. 2B). Based on the classification of DEGs in both LA1589 and M82, we found a large number of DEGs exhibited variable up- or down-regulation, while a small number of genes were commonly up- or down-regulated (Fig. 2C). More genes showed common down-regulation. In addition, there were 621 and 422 DEGs that showed complex patterns of change. These results indicated the dynamic expression of genes in response to HS.

We further performed Gene Ontology (GO) and KEGG analysis on these DEGs. In M82, the up-regulated genes were significantly enriched in biological processes related to response to heat/water deprivation and photosynthesis. Conversely, the down-regulated genes were significantly enriched in cytoplasmic translation, small GTPase-mediated signal transduction, response to far red light/oxidative stress, and related to photosystem (Fig. 2D, Fig. S4, Table S4-5). The up-regulated genes in M82 or LA1589 are enriched in protein processing in the endoplasmic reticulum and metabolism pathways (Fig. S4, Table S5). The commonly down-regulated genes in both LA1589 and M82 were significantly enriched in protein-chromophore linkage, photosynthesis, and response to light stimulus/cold/cadmium ion/cytokinin (Fig. 2D, Table S4-5). The DEGs with complex expression patterns shared by LA1589 and M82 were mainly enriched in protein folding, and response to heat/high light intensity/hydrogen peroxide (H_2O_2)/osmotic stress (Fig. 2D, Table S4-5). On the other hand, the complex pattern DEGs in LA1589 were significantly enriched in photosynthesis, nucleosome assembly, response to osmotic stress/wounding (Fig. 2D, Table S4). These results suggest that after HS, both LA1589 and M82 exhibited changes in gene expression involved in common and distinct pathways. We also performed separate GO and KEGG analyses for differentially expressed TFs, which revealed the regulatory role of TFs in response to multiple hormones and stresses, mainly plant hormone signaling, as well as growth and developmental cycle (Fig. S5-6).

Comparing differences in heat response genes of LA1589 and M82

To investigate the heat response mechanisms of LA1589 and M82, and identify their similarities and differences, we compared the specific and shared DEGs in both genotypes. We identified a total of 10,681 DEGs in LA1589 and 10,462 DEGs in M82. Further classification revealed that in LA1589, there were 586 protein-coding genes (PCGs) and 35 TFs among the complex-pattern genes. There were 5,123 up-regulated PCGs and 283 up-regulated TFs; and 4,377 down-regulated PCGs and 277 down-regulated TFs. In M82, there were 401 PCGs and 21 TFs among the complex pattern genes. There were 5,253 up-regulated PCGs and 295 up-regulated TFs; and 4,269 down-regulated PCGs and 233 down-regulated TFs (Fig. 3A). Using Venn diagrams, we illustrated the specific and common up-regulated or down-regulated genes in each genotype. LA1589 had 1,857 genes specifically up-regulated and 1,228 genes specifically down-regulated, while M82 had 1,916 genes specifically up-regulated and 1,021 genes specifically down-regulated. In addition, there were many DEGs that showed consistent up-regulation or down-regulation in both genotypes, with a few DEGs showing opposite regulation patterns between the two genotypes (Fig. 3B). By displaying the expression patterns of specifically up-regulated or down-regulated genes in a heatmap, we observed a large number of genes with increased expression, with the number of up-regulated genes exceeding that of down-regulated genes, especially in LA1589, where the changes in expression levels were more pronounced at each time point (Fig. 3C). The heatmap of shared up-regulated or down-regulated genes displayed a more complex expression pattern (Fig. 3D). Among the DEGs, we identified several known heat-responsive genes, such as *SlCPK28*, *SlHK2*, *SlBAG9* and *SlNAC1*, that were specifically up-regulated in LA1589, potentially contributing to its superior thermotolerance. Furthermore, our analysis revealed several novel TFs with early or continuous activation patterns in LA1589, suggesting their potential involvement in the regulation of thermotolerance (Table S6).

Comprehensive GO and KEGG enrichment analyses revealed that the genes specifically down-regulated in M82 were mainly associated with the chloroplast stroma/translation/envelope/thylakoid membrane, thylakoid, cytoplasmic translation, and ribosome (Fig. 3E, Fig. S7, Table S7-8). The specifically up-regulated genes in M82 were significantly enriched in protein binding, endopeptidase inhibitor activity, endosomes, cytosol, leaf senescence, protein processing in the endoplasmic reticulum, and MAPK signaling pathway (Fig. 3E, Fig. S7, Table S7-8). On the other hand, the genes specifically down-regulated in LA1589 showed significant enrichment in plasma membrane, circadian rhythm, citrate cycle and metabolism. The specifically up-regulated genes in LA1589 were significantly enriched in protein binding, poly(A) RNA binding, photosynthesis, and vesicular transport (Fig. 3E, Fig. S7, Table S7-8). Moreover, the up-regulated genes in both LA1589 and M82 were primarily associated with GO terms such as response to heat, mitochondria, zinc ion binding, unfolded protein binding, and integral component of the membrane. Conversely, the

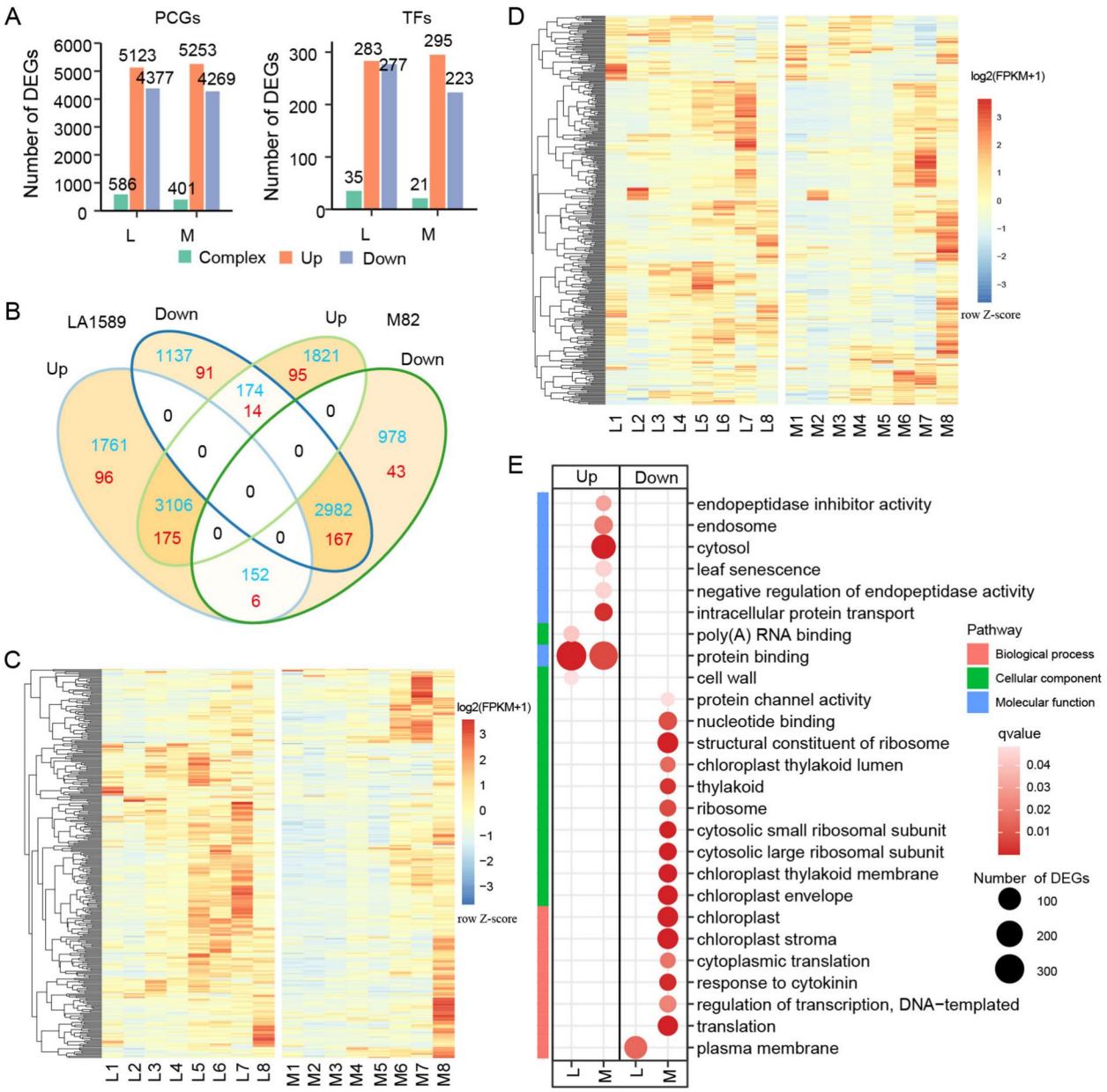


Fig. 3 Comparison of differentially expressed genes (DEGs) between LA1589 and M82 during heat stress and recovery. **A** Number of categorized DEGs in LA1589 and M82 after heat stress and recovery. DEGs includes protein-coding genes (PCGs) and transcription factors (TFs). Up, genes were up-regulated at least at one time point; Down, genes were down-regulated at least at one time point; Complex, genes were up-regulated at one time point but down-regulated at another. **B** Venn plots showing a comparison of genes that were up-regulated or down-regulated between LA1589 and M82 after heat stress and recovery. The numbers in red are for PCGs, and the numbers in blue are for TFs, **C** Heatmap showing expression profiles of specific up- and down-regulated genes in LA1589 and M82 as shown in (**B**). **D** Heatmap showing expression profiles of shared up- and down-regulated genes in LA1589 and M82 as shown in (**B**). **E** Representative gene ontology (GO) terms of specific up- and down-regulated genes in LA1589 and M82. The circle size indicates the number of DEGs associated with each GO term, with larger circles representing higher enrichment. The color intensity represents the q-value, with deeper red indicating greater reliability in the significance of DEG enrichment in the pathway. All significantly enriched GO terms (q-value < 0.05) at each time point are listed in Table S7

down-regulated genes in both genotypes were primarily enriched in GO terms related to photosystems, chloroplast photosynthesis, and responses to cytokinin, auxin, cadmium ions, and light (Fig. S8, Table S7). Our in-depth studies of specific up- and down-regulated TFs produced results consistent with those mentioned above (Fig. S9-10). These findings provide a deeper understanding of the shared and

distinct regulatory mechanisms employed by LA1589 and M82 under HS conditions.

Validation of DEGs using RT-qPCR

To validate the RNA-seq results, we performed RT-qPCR analysis on four DEGs, including *SlHSP20.1 SlHSP70*, *SlHSFA7* and *CPK28*. These genes are potential marker genes involved in HS (Hu et al. 2021; Su et al. 2023; Vu et al. 2023; Xu et al. 2024; Yu et al. 2016). Overall, the expression patterns of these four genes were consistent with the RNA-Seq results, confirming the reliability of the RNA-seq data obtained in this study. In most cases, LA1589 exhibited higher expression levels of these genes compared to M82, suggesting its superior tolerance to HS (Fig. 4).

Heat response gene modules identified using WGCNA

To further investigate the heat response regulatory network in LA1589 and M82, we assigned labels of 0 and 1 to the samples and physio-biochemical data generated in this study, respectively, and used them as phenotype values. We selected soft threshold values of 9 and 12, corresponding to R^2 values of 0.85 and 0.8 for WGCNA analysis, respectively (Fig. S11 A-B). Only genes with FPKM values ≥ 5 in at least one sample and with a high coefficient of variation (CV > 0.5) were included in the analysis. The results showed that the sample values and physio-biochemical indicators yielded 18 gene expression modules (labeled as TM1-TM18) and 23 gene expression modules (labeled as PM1-PM23), containing 13,392 and 16,863 genes, respectively (Fig. 5A–B).

We identified key modules for heat response based on PCC ≥ 0.5 and a P-value < 0.01. In these heat response modules, TM4 and TM11 are specifically associated with LA1589, while TM10, TM12, and TM16 are specifically associated with M82. TM11 is associated with time point L2, TM12 and TM10 are associated with time point M7, and M16 is associated with the recovery time point M8. Module TM3 is related to both LA1589 and M82 at the recovery time point, while TM6, TM7, TM8, and TM9 are positively correlated with LA1589 and negatively correlated with M82.

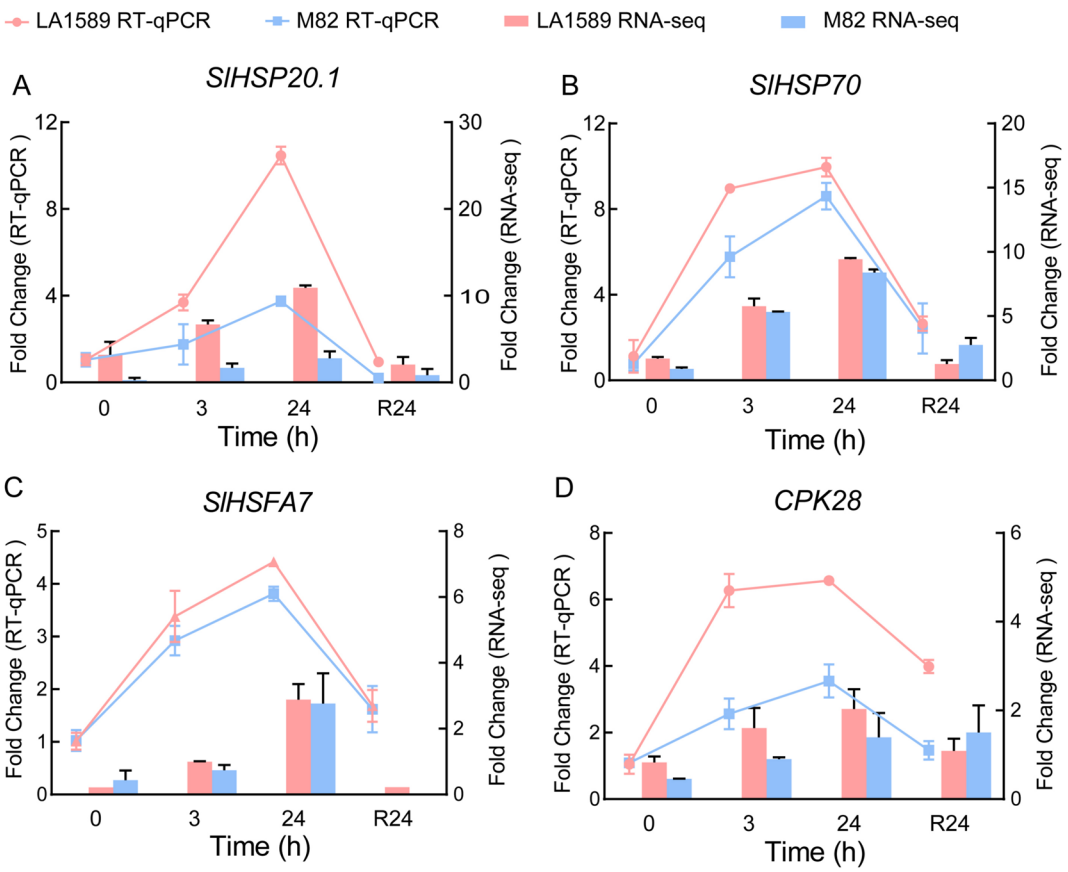


Fig. 4 Validation of transcriptome data by reverse transcription quantitative PCR (RT-qPCR). **A** *SlHSP20.1* (Solyc11g020040). **B** *SlHSP70* (Solyc09g065660). **C** *SlHSFA7* (Solyc02g083850). **D** *CPK28* (Solyc06g076540). Transcriptome and RT-qPCR data at 0, 3, and 24 h of heat treatment, followed by 24 h of recovery (R24) at room temperature, were log2 transformed. Data are presented as mean ± standard deviation of three biological replicates

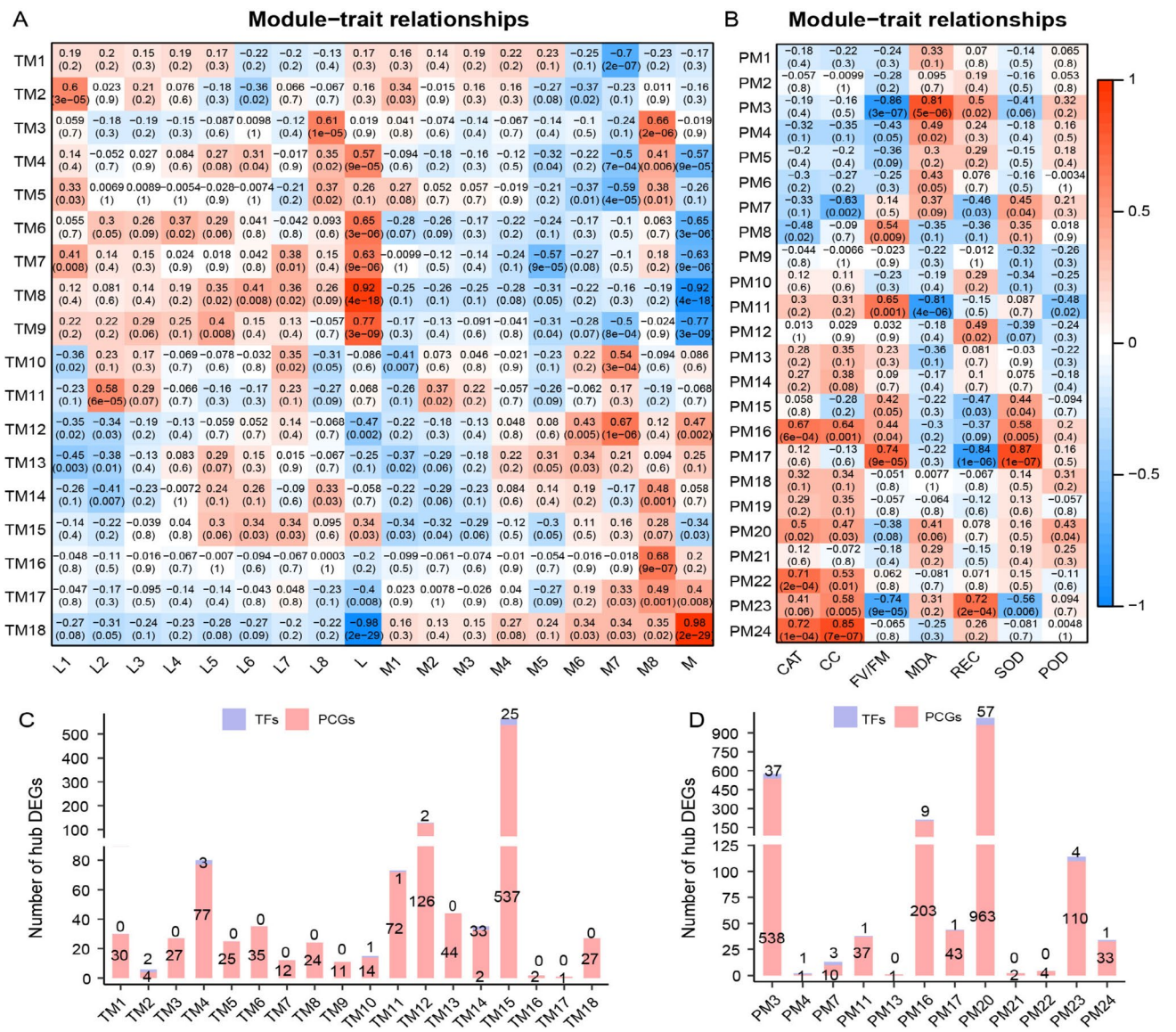


Fig. 5 Identification of co-expression modules using expressed genes under heat stress. **A** Module-time point correlation. The analysis yielded 18 gene expression modules (TM1-TM18). **B** Module and physio-biochemical index correlation. The analysis generated 23 gene expression modules (PM1-PM23). The X-axis corresponds to different time points and physio-biochemical indexes for LA1589 and M82 under heat stress, while the Y-axis represents each module. The colors represent the Pearson correlation coefficient (PCC), with negative correlations shown in blue and positive correlations shown in red. Darker indicate stronger correlations. **C** Number of hub DEGs in each co-expression module of TM. **D** Number of hub DEGs in each co-expression module of PM. Red and purple represent protein-coding genes (PCGs) and transcription factors (TFs), respectively

TM18 is positively correlated with M82 but negatively correlated with LA1589 (Fig. 5A). Furthermore, by correlating physio-biochemical indicators with modules, we found that module PM3 is related to the MDA content, PM8, PM11, and PM17 are related to the F_v/F_m value, and PM17 is also related to SOD activity. Modules PM16, PM22, and PM24 are related to both CAT activity and CC, and module PM23 is related to the REC value (Fig. 5B).

In addition, we extracted hub genes from each module based on the criterion of KME ≥ 0.9. The number of hub genes in modules TM1-TM18 ranged from 1 (TM17) to 562 (TM15), totaling 1,138 hub genes, including 36 TFs (Fig. 5C). For PM modules, the number of hub genes ranged from 0 (PM21 and PM22) to 1,020 (PM20), totaling 2,060 hub genes, including 114 TFs (Fig. 5D).

To determine whether the genes within these modules are involved in heat-related BPs, we conducted GO enrichment analysis. The results showed that genes in module TM11 are significantly enriched in response to heat/high light intensity/H_2O_2, chaperone-mediated protein folding, protein

folding and heat acclimation. Genes in module TM10 are enriched in the response to heat and abscisic acid-activated signaling pathway, and genes in module TM6 are significantly enriched in processes related to photosynthesis, photosynthetic electron transport, photosystem II stabilization, ATP synthesis/hydrolysis coupled to proton transport and ATP metabolic processes (Fig. S11C, Table S9). For the PM modules, genes in module PM3 are significantly enriched in carbohydrate metabolic process and response to heat, while genes in PM11 and PM22 are significantly enriched in BPs related to photosynthesis and photosynthetic electron transport chain, and genes in PM23 are significantly enriched in BPs related to negative regulation of endopeptidase activity and chloroplast stroma (Fig. S11D, Table S10).

Heat-tolerant candidate genes identified by WGCNA

When plants experience HS, a large number of genes undergo rapid change in expression. The early-responsive genes are particularly crucial. Based on this premise, we initially investigated the gene module TM11, which exhibited specific expression at the first time point (L2) under HS. Interestingly, TM11 module is specifically related to LA1589. Subsequently, we constructed a co-expression network consisting of genes within this module. Our analysis revealed that 73 hub genes in the TM11 expression network demonstrated a strong response to HS during the initial two time points, with significantly up-regulated expression (Fig. 6A–B, Table S11). Among these genes, we noticed a TF, Solyc09g065660, named *SlHsfA7* which encodes an A3-type of HSF. This TF is well-known for its involvement in the tomato HS response (Mesihovic et al. 2022). In addition, by constructing a heatmap, we displayed the top 10 genes with the highest connectivity in this network, with Solyc11g066100 positioned at the center. We observed that these 10 genes exhibited significant up-regulation in expression at time points L2, L3, M2, and M3, with the genes encoding heat shock proteins showing particularly pronounced differential expression (Fig. 6C).

Given the close relationship between CC, REC, and plant heat tolerance, we further explored the gene module PM23, which is significantly associated with CC and REC. The co-expression network within this module comprised 114 hub genes, including four TFs: LIM, AP2/ERF-ERF, GRAS, and Tify (Fig. 6D, Table S12). The genes within this module exhibited up-regulated expression at various time points after HS, with most of them functionally annotated as being related to chloroplasts (Fig. 6E, Table S12). Further analysis of the top 10 genes with the highest connectivity in this network led us to identify Solyc06g006080, which encodes thiamine biosynthesis protein ThiC and is homologous to *AtTHIC*, a gene in Arabidopsis encoding a thiamine biosynthetic protein and involved in chloroplast development (Kong et al. 2008). In addition, Solyc03g026130 was identified in this network, which encodes a cytochrome P450, a vital class of oxidases in plants (Fig. 6F). The highly interconnected expression of these genes within the network suggests their significant regulatory role in responding to HS.

Discussion

Climate change has led to HS becoming a significant challenge, with negative impacts on crop growth at different developmental stages. Tomato plants are sensitive to high temperatures, and even mild HS can reduce yield and quality, while more severe stress can lead to plant death (Jagadish et al. 2021). Therefore, identifying heat-tolerant genes, breeding superior varieties, and enhancing tomato resilience to high temperatures are effective strategies for adapting to climate change and improving yields. This study compared heat-related physiological and biochemical indicators between seedlings of the heat-tolerant genotype LA1589 and the heat-sensitive genotype M82, and identified a set of candidate heat-tolerant genes through dynamic transcriptome analysis in response to HS.

Under HS, tomato plants display symptoms including wilting, stunted growth, and developmental abnormalities (Wahid et al. 2007). Phenotypic screening is an intuitive approach for identifying heat-tolerant genotypes, with studies indicating that heat-resistant tomato varieties outperform heat-sensitive ones under stress conditions by exhibiting less wilting and higher survival rates (Bhattarai et al. 2021; Shaheen et al. 2016). In our study, LA1589 demonstrated less wilting than M82 after 24 h of HS and essentially returned to normal, whereas M82 continued to exhibit wilting symptoms, suggesting that LA1589 recovers from HS more effectively than M82.

Antioxidant enzymes such as SOD, POD, and CAT play a crucial role in detoxifying ROS and are essential components of HS adaptation. Plants enhance the activity of antioxidant enzymes to eliminate ROS generated under stress conditions, and their activity is positively correlated with heat tolerance. Heat-tolerant genotypes typically exhibit stronger antioxidant enzyme activity under HS (Lee et al. 2022; Kumar et al. 2017; Ahammed et al. 2019). In our study, although the POD activity in LA1589 was only slightly higher than that in M82 after stress, the activities of SOD and CAT were significantly higher in LA1589 compared to M82 at both the beginning and end of heat treatment. This indicates that LA1589 has a stronger ability to remove ROS than M82 (Fig. 1B–D), further supporting the idea that LA1589 has a stronger tolerance to high temperatures. Relative electrical conductivity reflects the stability of plant cell membranes under abiotic stress and serves as an important indicator of stress tolerance. Previous studies have

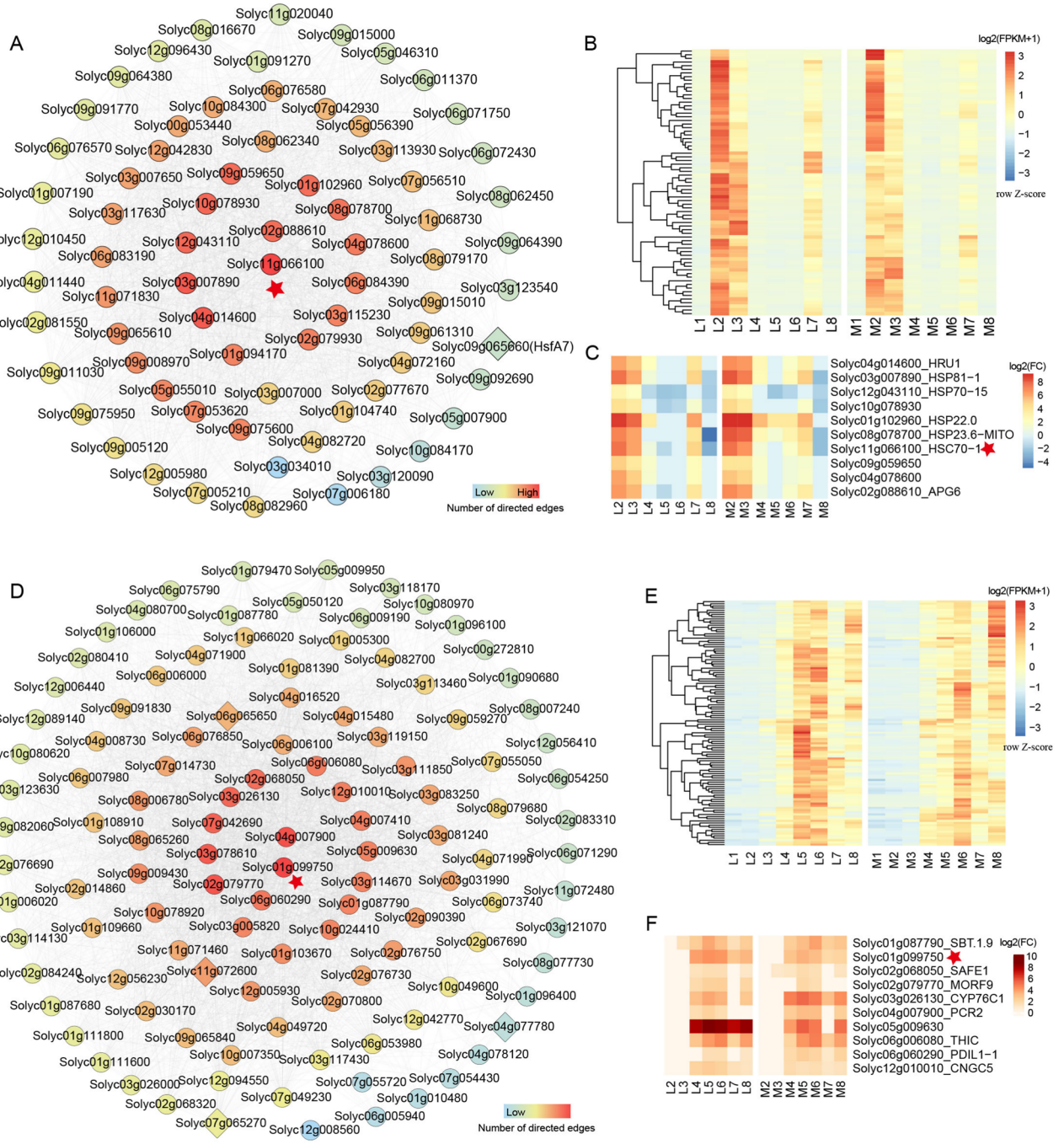


Fig. 6 Co-expression networks of heat response modules in LA1589 and M82. **A** Network illustrating connections between hub genes in the module TM11. **B** Expression levels of hub genes in TM11. **C** Expression changes of 10 hub genes in TM11. **D** Network illustrating connections between hub genes in the module PM23. **E** Expression levels of hub genes in PM23. **F** Expression changes of 10 hub genes in PM23. Each colored circle (node) represents one gene. Diamond shapes represent transcription factors (TFs). The red node color indicates higher connectivity within the network. Only edge correlations value (PCC $\geq$0.8) was shown

demonstrated the efficacy of utilizing leaf electrolyte leakage to identify heat-tolerant genotypes, with heat-resilient varieties typically exhibiting lower electrolyte leakage levels at elevated temperatures (Liu et al. 2023). Adverse stress conditions often result in secondary oxidative stress, leading to membrane lipid peroxidation. MDA is a key byproduct of membrane lipid peroxidation and offers insights into the extent of membrane damage in plants. Both REC and MDA levels in tomato plants under high temperature stress are effective indicators for screening heat tolerance (Karkute

et al. 2021). Our results showed that following the peak REC levels during the initial stage of HS, both genotypes experienced a decline, with the level of REC in M82 plateauing while that in LA1589 continued to decrease, suggesting that LA1589 exhibited stronger membrane stability and repair capabilities than M82 (Fig. 1E). In addition, at the onset of HS, LA1589 showed minimal change in MDA content, whereas M82 displayed a significant increase. By the end of the HS period, the rise in MDA content in LA1589 was notably lower than that in M82, further supporting that LA1589 is superior in detoxification under HS conditions (Fig. 1F).

Photosystem II (PSII) is highly vulnerable to HS, with chlorophyll fluorescence parameters (F_v/F_m) serving as a sensitive indicator of PSII photoinhibition (Baker 2008; Bhattarai et al. 2021; Sharma et al. 2015). Our study showed that both LA1589 and M82 exhibited reduced F_v/F_m under HS; however, PSII damage in M82 was more severe and its recovery ability was weaker compared to LA1589 (Fig. S1). In addition, the ability of tomato plants to maintain their greenness or delay senescence is also an important indicator of heat tolerance. Heat-sensitive tomato plants show a faster decline in the CC under high temperatures, leading to premature yellowing and wilting (Sharma et al. 2015). Our data showed that initially, LA1589 exhibited an increase in CC, suggesting an adaptation of the heat-tolerant genotype to high temperatures. When the plants were subjected to early HS, CC showed an increasing trend, providing thermal stability to PSII. Maintaining CC under high temperatures may be a characteristic of heat-tolerant tomato varieties. In our study, although CC initially increased, it gradually decreased with prolonged HS, leading to weakened photosynthesis, in line with previous research (Herde et al. 1999). Our data showed that the total CC of LA1589 was significantly higher than that of M82 at 6 h and 12 h of HS. In M82, the decrease in total CC led to a reduction in its photosynthetic efficiency, compromising its resistance to HS. In addition, the CC of LA1589 was consistently higher than that of M82 at different time points under HS, indicating that LA1589 has a stronger ability to maintain photosynthesis compared to M82 (Fig. 1G).

Plant adaptation to HS involves extensive transcriptional reprogramming to maintain normal growth and development under thermal challenges (Su et al. 2023). Our transcriptomic profiling revealed temporally dynamic differential gene expression between LA1589 and M82 under HS (Fig. 2B, Fig. S3), demonstrating that tomato plants undergo extensive changes in gene expression to adapt to HS. The identified DEGs are involved in photosynthesis, chlorophyll synthesis, and responses to temperature and light, as well as in membrane transport and protein folding (Fig. 2D), which are related to heat tolerance. Our research also focused on identifying TFs in tomato that show unique responsiveness to HS (Fig. S5-6, Fig. S9-10). These TFs potentially regulate multiple hormone signaling pathways and metabolic processes, thereby enabling tomato plants to maintain their adaptation to HS. These results provide valuable resources for identifying key genes involved in heat response.

Heat shock proteins (HSPs), heat shock transcription factors (HSFs), and calcium signaling constitute fundamental components of plant heat tolerance (Hu et al. 2016; Qu et al. 2013). In this study, we validated our transcriptomic data using well-known heat-resistant genes, including *SlHSP20.1*, *SlHSP70* , *SlHSFA7* and *CPK28* (Fig. 4). Previous studies have implicated these genes in the positive regulation of heat tolerance in tomato (Hu et al. 2021; Rao et al. 2022; Wang et al. 2004; Zhong et al. 2013). Our RT-qPCR results were overall consistent with the transcriptomic results, supporting the reliability and accuracy of the RNA-seq data. Furthermore, we investigated the expression patterns of previously reported tomato heat tolerance genes within our transcriptomic dataset. The results revealed that many of these genes are heat-responsive, including *SlHSFA7*, *SlHSP70*, *SlEGY2*, *SlBAG9*, *SlNAC1*, *SlCPK28*, *SlHSFB1*, and *SlTFT6* (Table S3), which aligns with their roles in heat stress adaptation (Hu et al. 2021; Liang et al. 2015, 2023; Mesihovic et al. 2022; Rao et al. 2022; Roth et al. 2017; Xu et al. 2024; Zhang et al. 2022). This further supports the authenticity and robustness of our transcriptomic dataset. In addition to the known genes, our study also identified many novel TFs from families such as MYB, NAC, WRKY, and bZIP, characterized by an early response (< 3 h) or sustained expression (Table S6), which may regulate previously uncharacterized thermotolerance mechanisms. For example Solyc07g054630 which was significantly up-regulated in LA1589 during the early stage of heat treatment, Solyc08g065910 and Solyc09g065660, as well as the Solyc02g089520 which was strongly down-regulated. Collectively, these findings provide new genes for further exploration of the molecular mechanisms underlying heat tolerance in tomato.

Sensors on the cell membrane detect external signals and transmit them to the interior of the cell to induce changes in cell metabolism under HS (Luu and Maurel 2013). Light signals have a significant impact on plant growth and development, and HS interferes with the transmission of light signals. Signals of high temperature and light antagonize each other and control plant morphological changes (Tan et al. 2023). This study found that many DEGs involved in membrane transport and light signal transduction were either activated or inhibited under HS (Fig. 2D). Furthermore, high temperature stress often leads to misfolding of protein and aggregation, resulting in cellular dysfunction and death (Lu et al. 2021). HSPs are a class of proteins that are highly expressed under HS and function as conserved molecular chaperones. HSFs promote the correct folding in plant cells by regulating the synthesis of HSPs, preventing aggregation, and enhancing cellular heat stability (Lang

et al. 2021; Nishad and Nandi 2021). TFs are important regulators of gene expression, recognizing and binding to regulatory elements in the promoter regions of target genes to activate or suppress transcription, thus participating in the response to HS (Liu et al. 2020b). Gaining a deeper understanding of the gene regulatory network in tomato under HS can contribute to the development of heat-tolerant tomato varieties to ensure yield and quality. From the WGCNA results, we noticed that the TF, Solyc09g065660 (*SlHsfA7*), encoding HS transcription factor A3, showed significant up-regulation under HS in the gene co-expression network of the TM11 module (Fig. 6A–C). Previous studies have shown that *SlHsfA7* is involved in regulating tomato heat tolerance (Mesihovic et al. 2022). Another hub gene in this co-expression network, Solyc02g088610 (*LeHSP100*), is responsive to salt stress. Recent studies have further shown that the gene *LeHSP100* is involved in the regulation of a heat stress-responsive network and may play a regulatory role under HS by interacting with four HSFs (Graci et al. 2024) Interestingly, the top ten connectivity genes in this module are related to various types of HSPss, including the HSP70, HSP23, HSP20, and HSP90, and the expression levels of these genes change dramatically at the beginning of HS (Fig. 6C). Previous studies uncovered a complex regulatory mechanism involving HSP90, HSP70 and three types of HSFs in controlling HS response (Hahn et al. 2011). This suggests that *SlHsfA7* may regulate the response of tomato to HS by modulating these HSPs and other genes in this network.

CC and REC play important roles in the plant's response to HS. The WGCNA results revealed a significant correlation between the PM23 gene module and these indicators (Fig. 5B), suggesting that genes in this module are involved in regulating tomato heat tolerance. Further GO enrichment analysis found that genes in this module are significantly enriched in many BPs related to heat response and photosynthesis (Fig. S11D), supporting the potential role of this module in regulating tomato heat tolerance. These genes were up-regulated at multiple time points after HS, suggesting they may play a role in heat adaptation. Of particular interest is Solyc06g006080, encoding thiamine biosynthesis protein ThiC, a key enzyme involved in chloroplast development (Kong et al. 2008). Before heat treatment, no significant difference in Thic expression was observed between the two genotypes. However, during HS, this gene exhibited a continuous upregulation trend in LA1589, while in M82, expression initially decreased before increasing. After 6 h of heat treatment, the expression level of ThiC in LA1589 was significantly higher than in M82 (Fig. 6F, Table S3). This genotype-specific upregulation suggests a role for ThiC in stabilizing chloroplast integrity under HS. Additionally, Solyc03g026130 encodes cytochrome P450, an important class of oxidoreductases in plants (Fig. 6D–F, Table S9). The regulation of these genes may play an important role in maintaining chloroplast function and redox balance in plants under HS. The expression of Solyc05g009630, encoding a disease resistance protein, was significantly induced in LA1589 under HS. High temperature conditions can potentially impair plant resistance to disease by accelerating plant cell metabolism and disrupt function of resistant proteins (Hua and Dong 2022). Consequently, Solyc05g009630 may play a pivotal role in the plant's response to HS. Our findings indicate that while the expression of Solyc05g009630 showed an initial increase followed by a decline in both genotypes, its induction in LA1589 was substantially greater than in M82 during HS (Table S3). Previous studies have demonstrated that inhibition of *SlEGY2* (Solyc06g019200) expression results in reduced chlorophyll content, photosynthetic activity and electrolyte leakage, resulting in diminished heat resistance (Zhang et al. 2022). In our study, *SlEGY2* are no significant difference between the two genotypes in the early stage of heat treatment, but as the heat treatment progressed (0.5–12 h), *SlEGY2* expression in LA1589 showed persistent up-regulation, while in M82, it was significantly down-regulated (Table S3). The above results also reflect the superiority of LA1589 in maintaining photosynthesis under HS. Overall, this study identified several key genes related to heat regulation in tomato plants based on the gene co-expression network, which may play important roles in the regulation of photosynthesis under HS in tomato plants (Fig. 6F). In the future, we aim to carry out functional and mechanistic studies on these genes to unveil the molecular mechanisms underlying heat tolerance in tomato, and thus to improve tomato survival and yield in high temperature environments.

Differences in heat tolerance exist among tomato varieties, and these differences may be caused by genetic variations in the genome (Bineau et al. 2021). In this study, we detected differences in gene response to HS between the heat-tolerant genotype LA1589 and the heat-sensitive genotype M82. Specifically, in addition to finding that some genes were up- or down-regulated in both genotypes under HS, a large number of genes were specifically up- or down-regulated in each genotype (Fig. 3B). These differences may be due to variations in genetic regulation between varieties. GO enrichment results based on specifically expressed genes revealed significant enrichment of down-regulated genes related to chloroplast processes in M82, possibly indicating that the response to HS may be mediated by regulating chloroplast function. Meanwhile, the down-regulated genes in LA1589 were significantly enriched in the plasma membrane pathway, suggesting that they may play an important role in maintaining cell membrane integrity and cellular homeostasis (Fig. 3E). These results suggest that heat-tolerant LA1589 and heat-sensitive M82 exhibit differences in gene pathways and regulatory mechanisms associated with

HS. Furthermore, the WGCNA results identified key heat response modules associated with specific tomato genotypes and time points. These modules likely represent genotype-specific heat response mechanisms. Specifically, modules TM4 and TM11 were associated with tomato LA1589, while modules TM10, TM12, and TM16 were associated with tomato M82 (Fig. 5).

Understanding the function and regulatory networks of genes in these modules will provide insights into how tomato plants regulate gene expression to adapt to high-temperature environments and offer important guidance for genetic improvement of heat tolerance.

Conclusion

Our findings demonstrated the superior heat tolerance of LA1589 compared to M82 at the seedling stage, which is characterized by higher antioxidant capacity, the maintenance of chlorophyll content and photosynthetic capacity, and less damage to the plant. Furthermore, our study provides valuable insights into the underlying genetic and regulatory networks involved in heat stress response, laying the foundation for future investigations into the precise functions and molecular mechanisms of genes in specific modules involved in heat adaptation.

Supplementary Information The online version contains supplementary material available at https://doi.org/10.1007/s10725-025-01322-6.

Author contributions Chunmei Shi: Data curation, Formal analysis, Visualization and Writing—original draft. Bo Liu: Data curation, Formal analysis, Visualization and Writing—original draft. Lei Song: Investigation. Yunfei Tang: Investigation. Jiawei Chen: Investigation. Xinyan Shen: Investigation. Yuxin Peng: Investigation. Can Yang: Investigation. Guangyu Lu: Investigation. Xuan Deng: Investigation. Yongen Lu: Writing—review & editing. Michal Lieberman-Lazarovich: Conceptualization, Writing—review & editing. Bo Ouyang: Conceptualization, Project administration, Supervision, and Writing—review & editing.

Funding This work was supported by the National Key Research and Development Program of China (2022YFE0100900), and the National Natural Science Foundation of China (31972416, U1906205, U21A20230) and the Earmarked Fund for China Agriculture Research System (CARS-23-A13).

Data availability The authors declare that the gene expression file has been deposited in Zendo (https://zenodo.org/records/10449833) and the remaining data supporting the findings of this study are available in the paper and Supplemental information.

Declarations

Conflict of interest The authors declare no competing interests.

Ethical approval Our study was conducted in full compliance with local regulations. This article did not involve any studies with human, animals, or endangered species. The collection of plant materials and the experimental procedures conducted in this study adhered to institutional, national and international guidelines and legal requirements.

Consent for publication Not applicable.

Open Access This article is licensed under a Creative Commons Attribution-NonCommercial-NoDerivatives 4.0 International License, which permits any non-commercial use, sharing, distribution and reproduction in any medium or format, as long as you give appropriate credit to the original author(s) and the source, provide a link to the Creative Commons licence, and indicate if you modified the licensed material. You do not have permission under this licence to share adapted material derived from this article or parts of it. The images or other third party material in this article are included in the article's Creative Commons licence, unless indicated otherwise in a credit line to the material. If material is not included in the article's Creative Commons licence and your intended use is not permitted by statutory regulation or exceeds the permitted use, you will need to obtain permission directly from the copyright holder. To view a copy of this licence, visit http://creativecommons.org/licenses/by-nc-nd/4.0/.

References

Ahammed GJ, Xu W, Liu AR, Chen SC (2019) Endogenous melatonin deficiency aggravates high temperature-induced oxidative stress in *Solanum lycopersicum* L. Environ Exp Bot 161:303–311. https://doi.org/10.1016/j.envexpbot.2018.06.006

Aldubai AA, Alsadon AA, Migdadi HH, Alghamdi SS, Al-Faifi SA, Afzal M (2022) Response of tomato (*Solanum lycopersicum* L.) genotypes to heat stress using morphological and expression study. Plants (Basel) 11(5):615. https://doi.org/10.3390/plants11050615

Azameti MK, Ranjan A, Singh PK, Gaikwad K, Singh AK, Dalal M, Arora A, Rai V, Padaria JC (2022) Transcriptome profiling reveals the genes and pathways involved in thermo-tolerance in wheat (*Triticum aestivum* L.) genotype Raj 3765. Sci Rep-UK 12(1):14831. https://doi.org/10.1038/s41598-022-18625-7

Baker NR (2008) Chlorophyll fluorescence: a probe of photosynthesis in vivo. Annu Rev Plant Biol 59:89–113. https://doi.org/10.1146/annurev.arplant.59.032607.092759

Beyer WF, Fridovich I (1987) Assaying for superoxide-dismutase activity - some large consequences of minor changes in conditions. Anal Biochem 161(2):559–566. https://doi.org/10.1016/0003-2697(87)90489-1

Bhattarai S, Harvey JT, Djidonou D, Leskovar DI (2021) Exploring morpho-physiological variation for heat stress tolerance in tomato. Plants (Basel) 10(2):347. https://doi.org/10.3390/plants10020347

Bheemanahalli R, Sunoj VSJ, Saripalli G, Prasad PVV, Balyan HS, Gupta PK, Grant N, Gill KS, Jagadish SVK (2019) Quantifying the impact of heat stress on pollen germination, seed set, and grain filling in spring wheat. Crop Sci 59(2):684–696. https://doi.org/10.2135/cropsci2018.05.0292

Bineau E, Diouf I, Carretero Y, Duboscq R, Bitton F, Djari A, Zouine M, Causse M (2021) Genetic diversity of tomato response to heat stress at the QTL and transcriptome levels. Plant J 107(4):1213–1227. https://doi.org/10.1111/tpj.15379

Bita CE, Gerats T (2013) Plant tolerance to high temperature in a changing environment: scientific fundamentals and production of heat stress-tolerant crops. Front Plant Sci 4:273. https://doi.org/10.3389/fpls.2013.00273

Bu DC, Luo HT, Huo PP, Wang ZH, Zhang S, He ZH, Wu Y, Zhao LH, Liu JJ, Guo JC, Fang SS, Cao WC, Yi L, Zhao Y, Kong

L (2021) KOBAS-i: intelligent prioritization and exploratory visualization of biological functions for gene enrichment analysis. Nucleic Acids Res 49(W1):W317–W325. https://doi.org/10.1093/nar/gkab447

Cao WH, Liu J, He XJ, Mu RL, Zhou HL, Chen SY, Zhang JS (2007) Modulation of ethylene responses affects plant salt-stress responses. Plant Physiol 143(2):707–719. https://doi.org/10.1104/pp.106.094292

Chakraborty K, Singh AL, Kalariya KA, Goswami N, Zala PV (2015) Physiological responses of peanut (*Solanum lycopersicum* L.) cultivars to water deficit stress: status of oxidative stress and antioxidant enzyme activities. Acta Bot Croat 74(1):123–142. https://doi.org/10.1515/botcro-2015-0011

Chen S, Zhou Y, Chen Y, Gu J (2018) fastp: an ultra-fast all-in-one FASTQ preprocessor. Bioinformatics 34(17):i884–i890. https://doi.org/10.1093/bioinformatics/bty560

Choudhary AK, Thakur SK, Suri VK (2013) Technology transfer model on integrated nutrient management technology for sustainable crop production in high-value cash crops and vegetables in northwestern himalayas. Commun Soil Sci Plan 44(11):1684–1699. https://doi.org/10.1080/00103624.2013.783058

Doncheva NT, Morris JH, Gorodkin J, Jensen LJ (2019) Cytoscape stringapp: network analysis and visualization of proteomics data. J Proteome Res 18(2):623–632. https://doi.org/10.1021/acs.jproteome.8b00702

Driedonks N, Wolters-Arts M, Huber H, de Boer GJ, Vriezen W, Mariani C, Rieu I (2018) Exploring the natural variation for reproductive thermotolerance in wild tomato species. Euphytica 214(4):67. https://doi.org/10.1007/s10681-018-2150-2

Graci S, Cigliano RA, Barone A (2024) Exploring the gene expression network involved in the heat stress response of a thermotolerant tomato genotype. BMC Genomics 25(1):509. https://doi.org/10.1186/s12864-024-10393-0

Hahn A, Bublak D, Schleiff E, Scharf KD (2011) Crosstalk between HSP90 and HSP70 chaperones and heat stress transcription factors in tomato. Plant Cell 23(2):741–755. https://doi.org/10.1105/tpc.110.076018

Hedhly A (2011) Sensitivity of flowering plant gametophytes to temperature fluctuations. Environ Exp Bot 74:9–16. https://doi.org/10.1016/j.envexpbot.2011.03.016

Herde O, Pena Cortes H, Wasternack C, Willmitzer L, Fisahn J (1999) Electric signaling and pin2 gene expression on different abiotic stimuli depend on a distinct threshold level of endogenous abscisic acid in several abscisic acid-deficient tomato mutants. Plant Physiol 119(1):213–218. https://doi.org/10.1104/pp.119.1.213

Hu ZJ, Lv XZ, Xia XJ, Zhou J, Shi K, Yu JQ, Zhou YH (2016) Genome-wide identification and expression analysis of calcium-dependent protein kinase in tomato. Front Plant Sci 7:469. https://doi.org/10.3389/fpls.2016.00469

Hu T, Wang Y, Wang Q, Dang N, Wang L, Liu C, Zhu J, Zhan X (2019) The tomato 2-oxoglutarate-dependent dioxygenase gene *SlF3HL* is critical for chilling stress tolerance. Hortic Res 6:45. https://doi.org/10.1038/s41438-019-0127-5

Hu ZJ, Li JX, Ding ST, Cheng F, Li X, Jiang YP, Yu JQ, Foyer CH, Shi K (2021) The protein kinase CPK28 phosphorylates ascorbate peroxidase and enhances thermotolerance in tomato. Plant Physiol 186(2):1302–1317. https://doi.org/10.1093/plphys/kiab120

Hua J, Dong XN (2022) Sustaining plant immunity in rising temperature. Cell Res 32(12):1038–1039. https://doi.org/10.1038/s41422-022-00710-1

Ikram M, Chen JF, Xia YS, Li RH, Siddique KHM, Guo PG (2022) Comprehensive transcriptome analysis reveals heat-responsive genes in flowering Chinese cabbage (*Brassica campestris* L. ssp. *chinensis*) using RNA sequencing. Front Plant Sci 13:1077920. https://doi.org/10.3389/fpls.2022.1077920

IPCC, 2023: Climate Change 2023: Synthesis Report. Contribution of Working Groups I, II and III to the Sixth Assessment Report of the Intergovernmental Panel on Climate Change [Core Writing Team, H. Lee and J. Romero (eds.)]. IPCC, Geneva, Switzerland, pp. 35–115, https://doi.org/10.59327/IPCC/AR6-9789291691647.

Jagadish SVK, Way DA, Sharkey TD (2021) Plant heat stress: concepts directing future research. Plant Cell Environ 44(7):1992–2005. https://doi.org/10.1111/pce.14050

Jagtap AB, Yadav IS, Vikal Y, Praba UP, Kaur N, Gill AS, Johal GS (2023) Transcriptional dynamics of maize leaves, pollens and ovules to gain insights into heat stress-related responses. Front Plant Sci 14:1117136. https://doi.org/10.3389/fpls.2023.1117136

Karkute SG, Ansari WA, Singh AK, Singh PM, Rai N, Bahadur A, Singh J (2021) Characterization of high-temperature stress-tolerant tomato (*Solanum lycopersicum* L.) genotypes by biochemical analysis and expression profiling of heat-responsive genes. 3 Biotech 11(2):45. https://doi.org/10.1007/s13205-020-02587-6

Kim D, Paggi JM, Park C, Bennett C, Salzberg SL (2019) Graph-based genome alignment and genotyping with HISAT2 and HISAT-genotype. Nat Biotechnol 37(8):907–915. https://doi.org/10.1038/s41587-019-0201-4

Kong D, Zhu Y, Wu H, Cheng X, Liang H, Ling HQ (2008) AtTHIC, a gene involved in thiamine biosynthesis in *Arabidopsis thaliana*. Cell Res 18(5):566–576. https://doi.org/10.1038/cr.2008.35

Kumar RR, Goswami S, Shamim M, Mishra U, Jain M, Singh K, Singh JP, Dubey K, Singh S, Rai GK, Singh GP, Pathak H, Chinnusamy V, Praveen S (2017) Biochemical defense response: characterizing the plasticity of source and sink in spring wheat under terminal heat stress. Front Plant Sci 8:1603. https://doi.org/10.3389/fpls.2017.01603

Lang BJ, Guerrero ME, Prince TL, Okusha Y, Bonorino C, Calderwood SK (2021) The functions and regulation of heat shock proteins; key orchestrators of proteostasis and the heat shock response. Arch Toxicol 95(6):1943–1970. https://doi.org/10.1007/s00204-021-03070-8

Langfelder P, Horvath S (2008) WGCNA: an R package for weighted correlation network analysis. BMC Bioinformatics 9:559. https://doi.org/10.1186/1471-2105-9-559

Lee K, Rajametov SN, Jeong HB, Cho MC, Lee OJ, Kim SG, Yang EY, Chae WB (2022) Comprehensive understanding of selecting traits for heat tolerance during vegetative and reproductive growth stages in tomato. Agronomy 12(4):834. https://doi.org/10.3390/agronomy12040834

Li H, Handsaker B, Wysoker A, Fennell T, Ruan J, Homer N, Marth G, Abecasis G, Durbin R, Proc GPD (2009) The sequence alignment/map format and SAMtools. Bioinformatics 25(16):2078–2079. https://doi.org/10.1093/bioinformatics/btp352

Liang XQ, Ma NN, Wang GD, Meng X, Ai XZ, Meng QW (2015) Suppression of *SlNAC1* reduces heat resistance in tomato plants. Biol Plant 59(1):92–98. https://doi.org/10.1007/s10535-014-0477-7

Liang YF, Ma F, Zhang RL, Li WY, Dang J, Su H, Li BY, Hu TX, Zhang MK, Liang Y, Zhan XQ (2023) Genome-wide identification and characterization of tomato 14–3–3(*SlTFT*) genes and functional analysis of *SlTFT6* under heat stress. Physiol Plantarum. 175(2):e13888. https://doi.org/10.1111/ppl.13888

Liao Y, Smyth GK, Shi W (2014) featureCounts: an efficient general purpose program for assigning sequence reads to genomic features. Bioinformatics 30(7):923–930. https://doi.org/10.1093/bioinformatics/btt656

Liu B, Song L, Deng X, Lu Y, Lieberman-Lazarovich M, Shabala S, Ouyang B (2023) Tomato heat tolerance: Progress and prospects. Sci Hortic 322:112435. https://doi.org/10.1016/j.scienta.2023.112435

Liu Y, Li J, Zhu Y, Jones A, Rose RJ, Song Y (2019) Heat stress in legume seed setting: effects, causes, and future prospects. Front Plant Sci 10:938. https://doi.org/10.3389/fpls.2019.00938

Liu GZ, Li CX, Yu HY, Tao PW, Yuan L, Ye J, Chen WF, Wang Y, Ge PF, Zhang JH, Zhou GL, Zheng W, Ye ZB, Zhang YY (2020a) *GREEN STRIPE*, encoding methylated TOMATO AGAMOUS-LIKE 1, regulates chloroplast development and Chl synthesis in fruit. New Phytol 228(1):302–317. https://doi.org/10.1111/nph.16705

Liu XH, Lyu YS, Yang W, Yang ZT, Lu SJ, Liu JX (2020b) A membrane-associated NAC transcription factor OsNTL3 is involved in thermotolerance in rice. Plant Biotechnol J 18(5):1317–1329. https://doi.org/10.1111/pbi.13297

Lohani N, Singh MB, Bhalla PL (2020) High temperature susceptibility of sexual reproduction in crop plants. J Exp Bot 71(2):555–568. https://doi.org/10.1093/jxb/erz426

Love MI, Huber W, Anders S (2014) Moderated estimation of fold change and dispersion for RNA-seq data with DESeq2. Genome Biol 15(12):1–21. https://doi.org/10.1186/s13059-014-0550-8

Lu S, Zhu T, Wang Z, Luo L, Wang S, Lu M, Cui Y, Zou B, Hua J (2021) Arabidopsis immune-associated nucleotide-binding genes repress heat tolerance at the reproductive stage by inhibiting the unfolded protein response and promoting cell death. Mol Plant 14(2):267–284. https://doi.org/10.1016/j.molp.2020.11.010

Luu DT, Maurel C (2013) Aquaporin trafficking in plant cells: an emerging membrane-protein model. Traffic 14(6):629–635. https://doi.org/10.1111/tra.12062

Mesihovic A, Ullrich S, Rosenkranz RRE, Gebhardt P, Bublak D, Eich H, Weber D, Berberich T, Scharf KD, Schleiff E, Fragkostefanakis S (2022) *HsfA7* coordinates the transition from mild to strong heat stress response by controlling the activity of the master regulator *HsfA1a* in tomato. Cell Rep 38(2):110224. https://doi.org/10.1016/j.celrep.2021.110224

Mizoi J, Todaka D, Imatomi T, Kidokoro S, Sakurai T, Kodaira KS, Takayama H, Shinozaki K, Yamaguchi-Shinozaki K (2023) The ability to induce heat shock transcription factor-regulated genes in response to lethal heat stress is associated with thermotolerance in tomato cultivars. Front Plant Sci 14:1269964. https://doi.org/10.3389/fpls.2023.1269964

Mubarok S, Ezura H, Anas K, Rostini N, Suminar E, Wiguna G (2019) Impacts of Sletr1-1 and Sletr1-2 mutations on the hybrid seed quality of tomatoes. J Integr Agr 18(5):1170–1176. https://doi.org/10.1016/s2095-3119(19)62614-6

Murchie EH, Lawson T (2013) Chlorophyll fluorescence analysis: a guide to good practice and understanding some new applications. J Exp Bot 64(13):3983–3998. https://doi.org/10.1093/jxb/ert208

Nishad A, Nandi AK (2021) Recent advances in plant thermomemory. Plant Cell Rep 40(1):19–27. https://doi.org/10.1007/s00299-020-02604-1

Pham D, Hoshikawa K, Fujita S, Fukumoto S, Hirai T, Shinozaki Y, Ezura H (2020) A tomato heat-tolerant mutant shows improved pollen fertility and fruit-setting under long-term ambient high temperature. Environ Exp Bot 178:104150. https://doi.org/10.1016/j.envexpbot.2020.104150

Qu AL, Ding YF, Jiang Q, Zhu C (2013) Molecular mechanisms of the plant heat stress response. Biochem Bioph Res Co 432(2):203–207. https://doi.org/10.1016/j.bbrc.2013.01.104

Rahmat BPN, Octavianis G, Budiarto R, Jadid N, Widiastuti A, Matra DD, Ezura H, Mubarok S (2023) *SlIAA9* mutation maintains photosynthetic capabilities under heat-stress conditions. Plants-Basel 12(2):378. https://doi.org/10.3390/plants12020378

Rajametov SN, Yang EY, Jeong HB, Cho MC, Chae SY, Paudel N (2021) Heat treatment in two tomato cultivars: a study of the effect on physiological and growth recovery. Horticulturae 7(5):119. https://doi.org/10.3390/horticulturae7050119

Rao S, Das JR, Balyan S, Verma R, Mathur S (2022) Cultivar-biased regulation of *HSFA7* and *HSFB4a* govern high-temperature tolerance in tomato. Planta 255(2):31. https://doi.org/10.1007/s00425-021-03813-y

Roth S, Mirus O, Bublak D, Scharf KD, Schleiff E (2017) DNA-binding and repressor function are prerequisites for the turnover of the tomato heat stress transcription factor *HsfB1*. Plant J 89(1):31–44. https://doi.org/10.1111/tpj.13317

Schmittgen TD, Livak KJ (2008) Analyzing real-time PCR data by the comparative CT method. Nat Protoc 3(6):1101–1108. https://doi.org/10.1038/nprot.2008.73

Shaheen MR, Ayyub CM, Amjad M, Waraich EA (2016) Morpho-physiological evaluation of tomato genotypes under high temperature stress conditions. J Sci Food Agric 96(8):2698–2704. https://doi.org/10.1002/jsfa.7388

Sharma DK, Andersen SB, Ottosen CO, Rosenqvist E (2015) Wheat cultivars selected for high F_v/F_m under heat stress maintain high photosynthesis, total chlorophyll, stomatal conductance, transpiration and dry matter. Physiol Plant 153(2):284–298. https://doi.org/10.1111/ppl.12245

Su HZ, Ma SY, Ma XH, Song Y, Wang XM, Cheng GX (2023) Transcriptome analyses show changes in heat-stress related gene expression in tomato cultivar "Moneymaker" under high temperature. J Plant Biochem Biot 32(2):328–337. https://doi.org/10.1007/s13562-022-00808-y

Tan W, Chen J, Yue X, Chai S, Liu W, Li C, Yang F, Gao Y, Gutiérrez Rodríguez L, Resco de Dios V, Zhang D, Yao Y (2023) The heat response regulators *HSFA1s* promote *Arabidopsis thermomorphogenesis* via stabilizing PIF4 during the day. Sci Adv 9(44):eadh1738. https://doi.org/10.1126/sciadv.adh1738

Vu NT, Nguyen NBT, Ha HH, Nguyen LN, Luu LH, Dao H, Vu TT, Huynh HTT, Le HTT (2023) Evolutionary analysis and expression profiling of the *HSP70* gene family in response to abiotic stresses in tomato (*Solanum lycopersicum*). Sci Progress-Uk 106(1):368504221148843. https://doi.org/10.1177/00368504221148843

Wahid A, Gelani S, Ashraf M, Foolad MR (2007) Heat tolerance in plants: an overview. Environ Exp Bot 61(3):199–223. https://doi.org/10.1016/j.envexpbot.2007.05.011

Wang WX, Vinocur B, Shoseyov O, Altman A (2004) Role of plant heat-shock proteins and molecular chaperones in the abiotic stress response. Trends Plant Sci 9(5):244–252. https://doi.org/10.1016/j.tplants.2004.03.006

Wang L, Feng Z, Wang X, Wang X, Zhang X (2010) DEGseq: an R package for identifying differentially expressed genes from RNA-seq data. Bioinformatics 26(1):136–138. https://doi.org/10.1093/bioinformatics/btp612

Wang K, Hersh HL, Benning C (2016) Sensitive to Freezing2 aides in resilience to salt and drought in freezing-sensitive tomato. Plant Physiol 172(3):1432–1442. https://doi.org/10.1104/pp.16.01183

Wen J, Jiang F, Weng Y, Sun M, Shi X, Zhou Y, Yu L, Wu Z (2019) Identification of heat-tolerance QTLs and high-temperature stress-responsive genes through conventional QTL mapping, QTL-seq and RNA-seq in tomato. BMC Plant Biol 19(1):398. https://doi.org/10.1186/s12870-019-2008-3

Xie DL, Huang HM, Zhou CY, Liu CX, Kanwar MK, Qi ZY, Zhou J (2022) *HsfA1a* confers pollen thermotolerance through upregulating antioxidant capacity, protein repair, and degradation in *Solanum lycopersicum* L. Hortic Res 9:uhac163. https://doi.org/10.1093/hr/uhac163

Xu T, Zhou H, Feng J, Guo MY, Huang HM, Yang P, Zhou J (2024) Involvement of HSP70 in BAG9-mediated thermotolerance in *Solanum lycopersicum*. Plant Physiol Bioch 207:108353. https://doi.org/10.1016/j.plaphy.2024.108353

Yu JH, Cheng Y, Feng K, Ruan MY, Ye QJ, Wang RQ, Li ZM, Zhou GZ, Yao ZP, Yang YJ, Wan HJ (2016) Genome-wide identification and expression profiling of tomato *HSP20* gene family in response to biotic and abiotic stresses. Front Plant Sci 7:1215. https://doi.org/10.3389/fpls.2016.01215

Yu W, Wang L, Zhao R, Sheng J, Zhang S, Li R, Shen L (2019) Knockout of *SlMAPK3* enhances tolerance to heat stress involving ROS homeostasis in tomato plants. BMC Plant Biol 19(1):354. https://doi.org/10.1186/s12870-019-1939-z

Zhang S, Chen C, Dai SS, Yang MM, Meng QW, Lv W, Ma NN (2022) A tomato putative metalloprotease *SlEGY2* plays a positive role in thermotolerance. Agriculture 12(7):940. https://doi.org/10.3390/agriculture12070940

Zhao C, Liu B, Piao SL, Wang XH, Lobell DB, Huang Y, Huang MT, Yao YT, Bassu S, Ciais P, Durand JL, Elliott J, Ewert F, Janssens IA, Li T, Lin E, Liu Q, Martre P, Müller C, Peng SS, Peñuelas J, Ruane AC, Wallach D, Wang T, Wu DH, Liu Z, Zhu Y, Zhu ZC, Asseng S (2017) Temperature increase reduces global yields of major crops in four independent estimates. PNAS 114(35):9326–9331. https://doi.org/10.1073/pnas.1701762114

Zheng Y, Yang Z, Luo J, Zhang Y, Jiang N, Khattak WA (2023) Transcriptome analysis of sugar and acid metabolism in young tomato fruits under high temperature and nitrogen fertilizer influence. Front Plant Sci 14:1197553. https://doi.org/10.3389/fpls.2023.1197553

Zhong LL, Zhou W, Wang HJ, Ding SH, Lu QT, Wen XG, Peng LW, Zhang LX, Lu CM (2013) Chloroplast small heat shock protein HSP21 interacts with plastid nucleoid protein pTAC5 and is essential for chloroplast development in *Arabidopsis* under heat stress. Plant Cell 25(8):2925–2943. https://doi.org/10.1105/tpc.113.111229

Zhou R, Yu XQ, Kjaer KH, Rosenqvist E, Ottosen CO, Wu Z (2015) Screening and validation of tomato genotypes under heat stress using F_v/F_m to reveal the physiological mechanism of heat tolerance. Environ Exp Bot 118:1–11. https://doi.org/10.1016/j.envexpbot.2015.05.006

Publisher's Note Springer Nature remains neutral with regard to jurisdictional claims in published maps and institutional affiliations.